Porous Gold Nanospheres by Controlled Transmetalation Reaction: A Novel Material for Application in Cell Imaging

Sourabh Shukla,[†] Anie Priscilla,[†] Meenal Banerjee,[‡] Ramesh R. Bhonde,[‡] J. Ghatak,[§] P. V. Satyam,[§] and Murali Sastry*,[†]

Nanoscience Group, Materials Chemistry Division, National Chemical Laboratory, Pune 411 008, India, National Center for Cell Sciences, Pune 411 007, India, and Institute of Physics, Bhuvaneshwar 751 005, India

Received June 1, 2005. Revised Manuscript Received August 4, 2005

Hollow shell nanostructures have numerous potential applications due to their interesting optical and electronic properties, which can be tuned by varying their shape, size, and shell thickness. In this paper we describe a simple galvanic replacement reaction (transmetalation reaction) involving sacrificial silver nanoparticles and Au(III) ions using a dialysis membrane. The dialysis membrane acts as a partial barrier that provides excellent control over the kinetics of reaction. This process results in the formation of porous gold nanospheres that improve the fluorescence in cell staining by offering an enhanced surface area for binding of the fluorescent dye, propidium iodide (PI). Such porous nanostructures could be ideal candidates for applications such as catalysis, enzyme immobilization, and drug delivery.

Introduction

Owing to their interesting shape and size dependent optical and electronic properties,[1] metal nanoparticles have fueled research in the fields of electronics,[2] optics,[3] clinical diagnostics,[4] sensors,[5] catalysis,[6] and therapeutics.[7] Bimetallic core−shell nanostructures constitute an interesting and well-studied subclass and have shown promise for application in catalysis.[8] Yet another special subset of metallic nanostructures is one in which the core is hollow. Hollow shell nanomaterials, apart from their unique optoelectronic properties,[9] have additional advantages of high specific surface area, low density, and cost-effectiveness that make them attractive catalysts.[10] Au hollow shells with absorption properties in the near-infrared (NIR) region have applications in cell imaging,[11] diagnostics, and plasmonics. Nanostructures with hollow interiors are generally prepared by depositing a thin layer of the shell material or their precursors on the surface of colloids (examples include gold, silver, ceramic, and polymeric beads) followed by selective removal of the core material by chemical etching or calcination.[12−16] Recently, the galvanic exchange reaction (transmetalation reaction) involving sacrificial metal nanoparticles and suitable metal ions has been employed by the Xia and Wan groups for forming hollow Au,[17] and Pt/AuPt[18] alloy nanostructures in water. Recently, Selvakannan and Sastry have demonstrated that hollow Au and Pt nanospheres may be synthesized by a similar transmetalation reaction in the organic phase.[19]

An understanding of the mechanism of hollow nanostructure formation via transmetalation reactions has been complicated by the fact that control over the rate of reaction, particularly at room temperature, has been difficult to achieve.[17] We demonstrate herein the use of a semipermeable dialysis tubing (normally used in biology for protein purification) to significantly slow and effectively control the transmetalation reaction between aqueous silver nanospheres and gold ions ($AuCl_4^-$) taken within and without the tubing, respectively. The pore size in the dialysis bag is smaller than the dimensions of the Ag nanoparticles (Ag NPs), thus resulting in infusion of gold ions into and effusion of silver ions produced due to the transmetalation reaction out of the

* Corresponding author. E-mail: sastry@ems.ncl.res.in.
[†] National Chemical Laboratory.
[‡] National Center for Cell Sciences.
[§] Institute of Physics.

(1) Jackson, J. B.; Westcott, S. L.; Hirsch, L. R.; West, J. L.; Halas, N, J. *Appl. Phys. Lett.* **2003**, *82*, 257.
(2) Chen, S.; Yang, Y. *J. Am. Chem. Soc.* **2002**, *124*, 5280.
(3) Brongersma, M. L.; Hartman, J. W.; Atwater, H. A. *Phys. Rev. B* **2000**, *62*, 356.
(4) Elghanian, R.; Stohoff, J. J.; Mucic, R. C.; Letsinger, R. L.; Mirkin, C. A. *Science* **1997**, *277*, 1078.
(5) Tkachenko, A. G.; Xie, H.; Coleman, D.; Glomm, W.; Ryan, J.; Anderson, M. F.; Franzen, S.; Feldheim, D. L. *J. Am. Chem. Soc.* **2003**, *125*, 4700.
(6) Mandal, S.; Roy, D.; Chaudhari, R. V.; Sastry, M. *Chem. Mater.* **2004**, *16*, 3714.
(7) Pankhurst, Q. A.; Connolly, J.; Jones, S. K.; Dobson, J. *J Phys D: Appl. Phys.* **2003**, *36*, R167−R181.
(8) Mandal, S.; Das, A.; Srivastava, R.; Sastry, M. *Langmuir* **2005**, *21*, 2408.
(9) Kociak, M.; Stéphan, O.; Henrard, L.; Charbois, V.; Rothschild, A.; Tenne, R.; Colliex, C. *Phys. Rev. Lett.* **2001**, *87*, 075501-1-075501-4.
(10) Kim, S. W.; Kim, M.; Lee, W. Y.; Hyeon, T. *J. Am. Chem. Soc.* **2002**, *124*, 7642.
(11) Chen, J.; Saeki, F.; Wiley, B.; Cang, H.; Cobb, M. J.; Li, Z.; Au, L.; Zhang, H.; Kimmey, M. J.; Li, X.; Xia, Y. *Nano Lett.* **2005**, *5*, 473.
(12) Chah, S.; Fendler, J. H.; Yi, J. *J. Colloid Interface Sci.* **2002**, *250*, 142.
(13) Caruso, F.; Caruso, R. A.; Mohwald, H. *Science* **1998**, *282*, 1111.
(14) Caruso, F.; Spasova, M.; Maceira, V.; Marzan, L. M. *Adv. Mater.* **2001**, *13*, 1090.
(15) Oldenburg, S. J.; Averitt, R. D.; Westcott, S. L.; Halas, N. J. *Chem. Phys. Lett.* **1998**, *248*, 243.
(16) Dhas, N. A.; Suslick, K. S. *J. Am. Chem. Soc.* **2005**, *127*, 2368.
(17) Sun, Y.; Xia, Y. *J. Am. Chem. Soc.* **2004**, *126*, 3892.
(18) (a) Liang, H.; Guo, Y.; Zhang, H.; Hu, J.; Wan, L.; Bai, C. *Chem. Commun.* **2004**, 1496. (b) Liang, H. P.; Wan, L. J.; Bai, C. L.; Jiang, L. *J. Phys. Chem. B* **2005**, *109*, 7795.
(19) Selvakannan, P. R.; Sastry, M. *Chem. Commun.* **2005**, 1684.

10.1021/cm051165f CCC: $30.25
Published on Web 09/03/2005

dialysis bag. This method not only provides excellent control over the reaction kinetics but also obviates the need for purification/separation procedures for the recovery of the porous nanostructures that has plagued earlier studies.[17] The use of a dialysis tubing to control the transmetalation reaction between sacrificial Ag NPs and gold ions results in the formation of highly porous gold nanospheres that we believe is due to controlled leaching out of silver atoms along defect directions in the Ag NPs. Recognizing that such porous nanospheres would have a significantly enhanced surface area relative to their solid counterparts, we show that the porous gold nanospheres are excellent candidates for cell imaging by conjugation with the commonly used fluorescent dye, propidium iodide (PI). PI is commonly used for imaging dead cells; interestingly, we observe that complexation with porous gold nanospheres enables their uptake by living cells as well. Hollow gold nanocages have been used to image cells by the technique "optical coherence tomography" (OCT).[11] The use of porous nanospheres conjugated with conventional, well-studied biological fluorophores considerably simplifies cell imaging and could have immediate application. Presented below are details of our investigation.

Experimental Details

Preparation of Ag NPs. Ag_2SO_4, tyrosine, KOH, and $HAuCl_4$ were obtained from Aldrich Chemicals and were used as-received. The synthesis of Ag NPs using tyrosine as a reducing agent under alkaline conditions was carried out as described elsewhere.[20] Briefly, 10 mL of aqueous Ag_2SO_4 (10^{-3} M) and 10 mL of tyrosine (10^{-3} M) were mixed in 70 mL of de-ionized water (Milli-Q, Elix 3) and the solutions were brought to boiling followed by addition of 10 mL of KOH (10^{-2} M) so as to achieve a final silver ion concentration of 10^{-4} M in solution. The color of the solution changed to yellow within a few minutes. The solution was allowed to cool to room temperature and dialyzed to remove excess KOH and unbound tyrosine before further use. The pH of the Ag NP solution was 7.5 following dialysis.

Transmetalation Reaction inside a Dialysis Membrane. A 12.5 kDa cutoff dialysis bag (Sigma Chemicals) was preprocessed to remove impurities as per the instruction given by the manufacturers. For the transmetalation experiment, 20 mL of aqueous Ag NP solution (pH 7.5) was taken in the dialysis bag and dialyzed against 200 mL of 5×10^{-5} M aqueous $HAuCl_4$ under constant stirring at room temperature for 48 h. The reaction between the Ag NPs and $AuCl_4^-$ ions was monitored by UV−Vis spectroscopy and transmission electron microscopy (TEM) analysis of the solutions inside and outside the dialysis bag periodically. Similar experiments were repeated by dialyzing the Ag NPs against 5×10^{-5} M $HAuCl_4$ using 2.5 and 30 kDa cutoff dialysis bags to study the effect of the dialysis tubing pore size on the reaction kinetics. Also, Ag NPs were dialyzed against 5×10^{-4} M $HAuCl_4$ to study the effect of concentration of Au(III) on the reaction kinetics. In another set of experiments, 5×10^{-5} and 5×10^{-4} M $HAuCl_4$ were added directly to the Ag NP solution and the reaction was monitored by UV−Vis spectroscopy.

UV−Vis Spectroscopy Measurements. UV−Vis spectra were recorded for all the solutions on a Jasco V-570 UV/Vis/NIR spectrophotometer operated at a resolution of 1 nm.

TEM Measurements. Samples for TEM analysis were prepared by drop-coating the Ag nanoparticle samples at various stages of transmetalation on carbon-coated copper grids. TEM measurements were performed on a JEOL model 1200EX instrument operated at an accelerating voltage of 80 kV. High-resolution TEM (HRTEM) measurements were also carried out on these nanoparticles on a JEOL-JEM-2010 UHR instrument operated at a lattice image resolution of 0.14 nm.

Cell Culture. Chinese hamster ovary (CHO) cells were cultured and maintained in tissue culture grade Nunclon flasks containing DMEM (Dulbecco's Modified Eagle Medium-Gibco, Grand Island, NY) supplemented with 10% FCS (Trace Biosciences PTY Ltd., New South Wales, Australia) and antibiotics (penicillin 200 U/mL and streptomycin 0.2 mg/mL) at 37 °C in a 5% CO_2 incubator.

Conjugation of PI with Porous Au NPs. Twenty-five mg/mL stock solution of propidium iodide (Sigma, St. Louis, MO) was prepared in phosphate buffer saline (PBS). 500 μL of the PI stock solution was added to 2 mL of porous gold and solid gold nanoparticle solutions. The porous gold NPs were prepared by the reaction of Ag NPs in a 12.5 kDa cutoff dialysis bag with 5×10^{-5} M $HAuCl_4$ solution as briefly described earlier while solid gold NPs were prepared by the sodium borohydride reduction of aqueous chloroauric acid solution as described elsewhere,[21] resulting in nanoparticles of size 6.5 ± 0.7 nm (TEM images in the Supporting Information, S1). Similarly 500 μL of PI was added to 2 mL of PBS as a control. These solutions were incubated for 3 h at room temperature under continuous stirring and then centrifuged at 14000 rpm for 30 min. While the supernatants were collected for fluorimetric analysis, the pellets thus obtained in each case were washed three times with PBS to remove unbound PI molecules (if any). The washed pellets were then resuspended in 100 μL of PBS and used for cell staining.

Quantification of PI Bound to the Nanoparticles. Fluorescence measurements of the supernatants collected from the porous and solid gold nanoparticle solutions were performed on a Fluoroskan Ascent fluorimeter by recording the emission at 590 nm after exciting the solutions at 485 nm. The difference in fluorescence intensities of the as-prepared PI solution and the supernatant after removal of the Au NPs after centrifugation was used as a measure to quantify the binding of PI to the porous and solid gold NPs.

Cell Fixation. The CHO cells were dislodged with trypsin, washed with PBS, pelleted down at 2000 rpm, and then fixed with 4% paraformaldehyde (w/v) in PBS (pH 7.2) for 10 min at 4 °C. This results in the death of the CHO cells. The fixed cells were then washed twice with PBS.

Cell Staining with PI-Labeled Au NPs and Confocal Microscopy Studies. The fixed CHO cells were subjected to RNase (5 mg/mL, USB, Amersham Life technologies, Cleveland, OH) treatment for 20 min at room temperature to avoid RNA contamination. The PI-labeled porous and solid Au NP solutions were then added to the cell suspensions and incubated at room temperature for 90 min in the dark. After incubation, the cells were washed with PBS to remove uncoordinated nanoparticle−PI conjugates. Stained as well as unstained cell preparations were cytospined (Shandon, cytospin 3) on glass slides and mounted with a fluorescent mounting medium. The slides were stored in the dark at 4 °C until analysis. For live cell staining, PI-labeled porous gold nanoparticles were incubated with live CHO cells at 37 °C for 30 min and the excess unbound PI−porous gold conjugates were washed away with PBS. These cells were then stained separately with Hoechst stain−33342 (12.5 μg/mL); this stain is conventionally used for live cell staining and was done to cross-check the uptake

(20) Selvakannan, P. R.; Swami, A.; Srisathiyanarayanan, D.; Shirude, P. S.; Pasricha, R.; Mandale, A. B.; Sastry, M. *Langmuir* **2004**, *20*, 7825.

(21) Patil, V.; Malvankar, R. B.; Sastry, M. *Langmuir* **1999**, *15*, 8197.

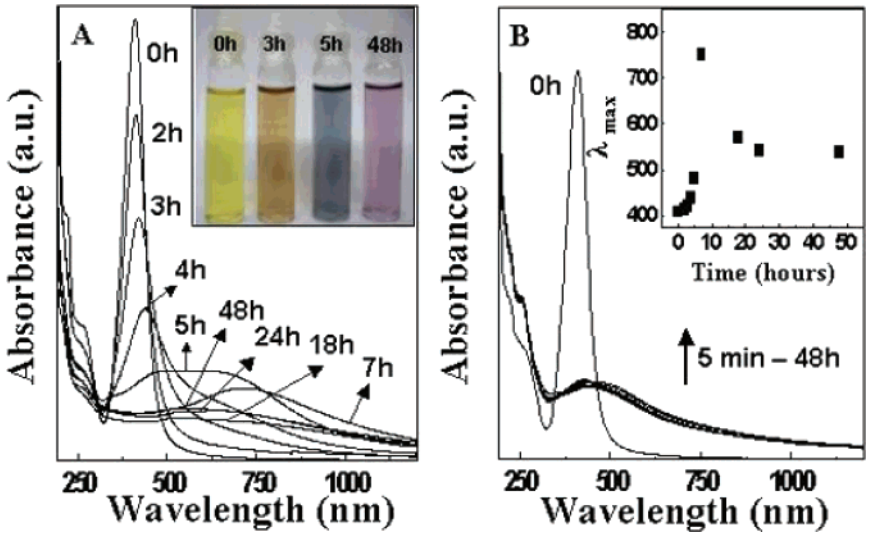

Figure 1. (A) UV−vis−NIR absorption spectra of Ag NPs in the dialysis bag as a function of time of reaction with 5×10^{-5} M $HAuCl_4$. The inset shows pictures of the Ag NP solution at different times of reaction. (B) UV−vis−NIR absorption spectra of Ag NPs directly reacted with 5×10^{-5} M $HAuCl_4$ solution. The inset is a plot of the Ag NP plasmon wavelength as a function of time of reaction (corresponding to spectra in A).

of PI-labeled porous gold nanospheres by the live cells and also to establish the viability of the cells after PI−porous gold treatment. After being washed with PBS, the cells were fixed and mounted as described previously. Similarly, live CHO cells were incubated with unconjugated pure PI to check the uptake of PI. All the images of the stained cells were recorded on an LSM 510 Zeiss workstation (Carl Zeiss Meditec AG, Jena, Germany) equipped with an argon air-cooled laser (LASOS Lasertechnik GmbH, Jena, Germany).

Results and Discussion

The galvanic replacement reaction between Au(III) and Ag NPs occurs since the standard reduction potential for the $AuCl_4^-$/Au pair (0.99 V vs standard hydrogen electrode, SHE) is higher than that of the Ag^+/Ag pair (0.80 V vs SHE). Thus, Ag NPs act as a sacrificial reducing agent in the reduction of Au(III) ions to Au^0 and in the process become oxidized to Ag^+. UV−vis−NIR spectra recorded from the Ag NP solution inside the dialysis bag (cutoff 12.5 kDa) as a function of time of reaction with 5×10^{-5} M aqueous $HAuCl_4$ solution are shown in Figure 1. As the reaction proceeds, damping of the silver plasmon absorption band centered at 408 nm, which shifts monotonically with time (up to 5 h of reaction) to ca. 480 nm (Figure 1B, inset), is observed. The progressive intensity decrease and red shift in the silver plasmon absorption band is symptomatic of loss of metallic silver via oxidation of the silver nanoparticles (to Ag^+) and formation of an Ag−Au alloy phase that becomes progressively rich in gold. At 5 h of reaction, an additional absorption band appears at 670 nm and indicates formation of a thin shell of gold on the sacrificial Ag nanoparticles.[22] After 7 h of reaction, a single broad absorption band centered at 750 nm appears (again consistent with a thin gold shell) which thereafter shifts to close to the surface plasmon band wavelength of Au (540 nm after 48 h of reaction; Figure 1A and inset of Figure 1B). During this reaction time scale, the color of the nanoparticle solution (inset of Figure 1A) changed from yellow (pure Ag NPs) to brown (3 h) to blue (5 h) and finally pink (48 h). The UV−vis−NIR spectroscopy observations are consistent with initial formation of an Ag−Au alloy phase (up to 5 h) that is followed by formation of a thin Au shell and finally by dealloying to yield Au NPs from the sacrificial Ag NPs. This is in agreement with the findings of Xia and co-workers who arrived at a similar mechanism based on direct reaction of different amounts of gold ions with silver nanocubes, nanowires, and spheres.[17] In the experiments by Xia et al., the transmetalation reaction was carried out at 100 °C and was complicated by the formation of an insoluble AgCl precipitate. The effusion of silver ions from the dialysis bag during transmetalation obviates this problem and provides a one-step procedure for obtaining pure Au NPs free of the oxidation product. Direct addition of 5×10^{-5} M $HAuCl_4$ solution to the Ag NPs results in the almost immediate reduction of the gold ions by the Ag NPs and formation of gold nanostructures well within 5 min of reaction (UV−vis−NIR absorption spectra in Figure 1B).

Representative transmission electron microscopy (TEM) images taken as a function of time of reaction of Ag NPs with 5×10^{-5} M $HAuCl_4$ solution (12.5 kDa dialysis bag cutoff) are shown in Figure 2. The as-prepared Ag NPs are predominantly spherical and range in size 40−50 nm (Figure 2A). Figure 3A shows a high-magnification TEM image of one of the as-prepared silver nanoparticles. The multiply twinned nature of the Ag NPs is seen in greater detail and the twin boundaries have been identified by arrows in this image. After 3 h of reaction, a large number of the Ag NPs show etching at specific locations on the particle surface and the creation of small voids (Figure 2B). Examination of one of the Ag NPs after 3 h of transmetalation reaction at higher magnification (Figure 3B) shows the topology of the voids much more clearly (indicated by arrows in the image). A comparison of Figures 3A and 3B strongly suggests that there is a correlation between the topology and position of the voids and the twins in the sacrificial silver nanoparticles. At this stage, the UV−vis−NIR spectra of the Ag NPs exhibited a peak at 419 nm, indicating a small percentage of gold in

(22) Oldenburg, S. J.; Jackson, J. B.; Westcott, S. L.; Halas, N. J. *Appl. Phys. Lett.* **1999**, *75*, 2897.

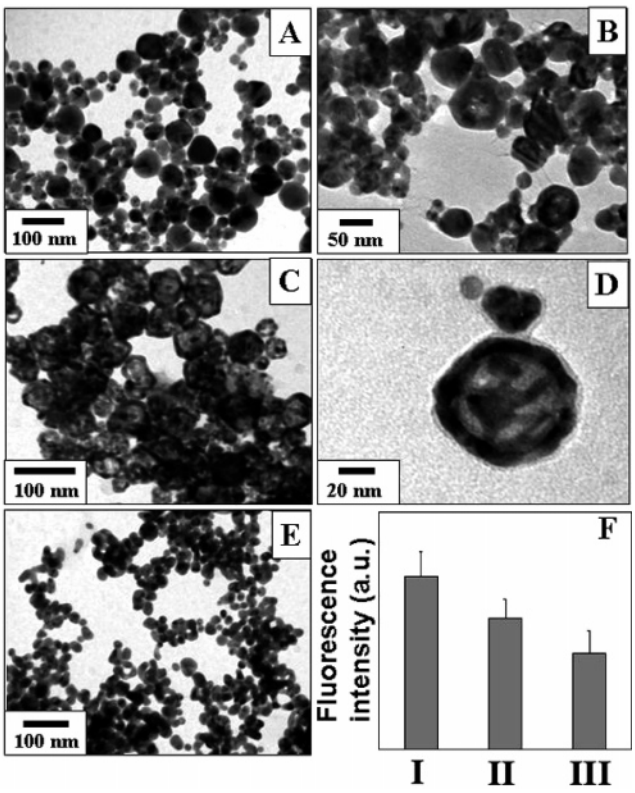

Figure 2. Representative TEM images of Ag NPs inside the dialysis bag as a function of time of reaction with 5×10^{-5} M $HAuCl_4$ solution: (A) 0 h, (B) 3 h, (C,D) 5 h, and (E) 48 h. (F) Fluorescence emission from PI in the supernatant after complexation with porous (III) and solid Au nanospheres (II). I corresponds to the fluorescence signal from pure unreacted PI (5 mg/mL).

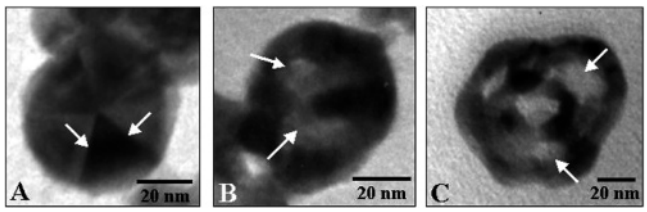

Figure 3. Representative high-magnification TEM images of Ag NPs inside the dialysis bag as a function of time of reaction with 5×10^{-5} M $HAuCl_4$ solution: (A) 0 h, (B) 3 h, and (C) 5 h. The arrows in A point to the twin boundaries on the surface of silver nanoparticles, which are the preferable site of leaching of silver as a result of the transmetalation reaction, leading to the formation of cavities (arrows in B and C).

the Ag−Au alloy. After 5 h of reaction, a much larger percentage of the Ag NPs show porosity with the size of the pores also increasing with time of reaction (Figures 2C and 2D). At higher magnification, one also observes that the number of pores per particle increases (Figure 3C) and that the position of the pores still bears a correlation with the multiply twinned structure of the starting sacrificial Ag NP (compare Figures 3A and 3C). The high-magnification TEM images shown in Figure 3 indicate that etching of the Ag NPs during the transmetalation reaction is initiated at the twin boundaries. The twin boundaries may also provide defect sites for facile effusion of the oxidized silver ions produced as the sacrificial Ag NPs are consumed in the reaction. The porous structures formed after 5 h of reaction are of a composition at the critical limit between alloying and dealloying (an alloy peak centered at 480 nm and a gold shell peak at 670 nm, UV−vis−NIR data in Figure 1).

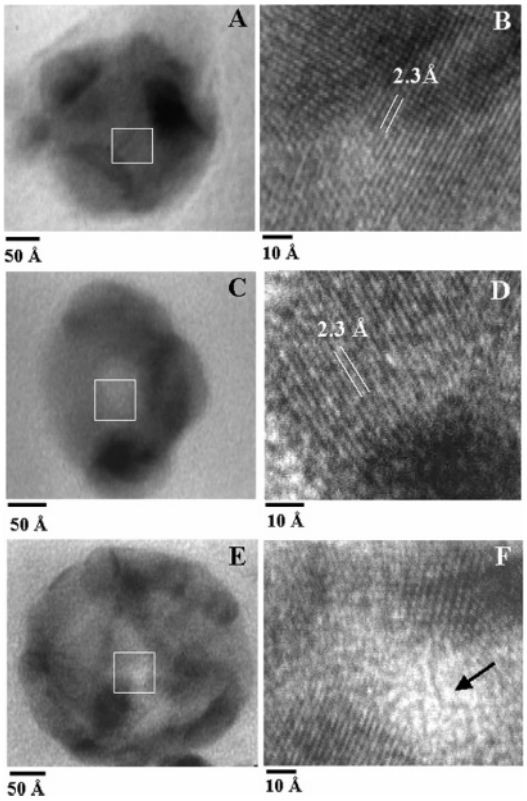

Figure 4. Representative HRTEM images at different magnifications recorded from the porous silver nanostructures after 2 h (A, B), 3 h (C, D), and 5 h of dialysis (E, F). Images B, D, and F correspond to magnified views of the regions indicated by the boxes in A, C, and E, respectively.

Further reaction with $AuCl_4^-$ ions leads to the formation of compact, spherical structures with little evidence of porosity, indicating collapse of the porous structure (Figure 2E). These particles are completely gold (broad peak centered at 537 nm, Figure 1A). The rate of transmetalation may be varied by either changing the cutoff of the dialysis bag or the concentration of $AuCl_4^-$ ions. An increase in the $HAuCl_4$ concentration to 5×10^{-4} M (12.5 kDa dialysis bag cutoff) and use of a dialysis bag of 30 kDa cutoff (5×10^{-5} M $HAuCl_4$ solution) both result in enhanced transmetalation reaction rates (Supporting Information, S2) and to porous structures similar to those seen in Figures 2C and 2D at much earlier times (Supporting Information, S2). While the TEM images discussed above suggest the formation of a porous structure, this evidence is not conclusive. HRTEM studies of the sacrificial silver nanospheres at various times of transmetalation reaction are shown in (Figure 4; A,B: 2 h, C,D: 3 h; E,F: 5 h). The presence of well-defined lattice planes in the core after 2 and 3 h of reaction indicates that the silver core is not completely oxidized at this stage of reaction (Figures 4A,B and 4C,D). After 5 h of reaction, however, there are regions (identified by an arrow in Figure 4F) in the porous structure that are free of fringes corresponding to lattice planes, indicating that these are indeed cavities. The *d* spacings in the HRTEM images shown in Figures 4B and 4D were determined to be 2.3 Å and correspond to the (1 1 1) lattice planes of either gold or silver. Energy dispersive analysis of X-rays (EDX) measurements carried out on the sacrificial silver nanoparticles in the HRTEM instrument after 2, 3, and 5 h of transmetalation

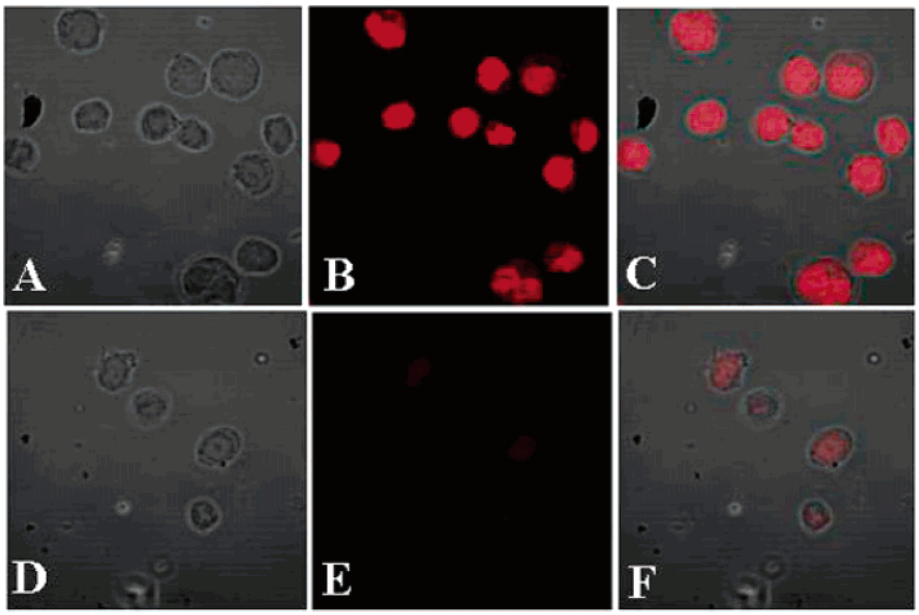

Figure 5. Confocal microscopy images of fixed CHO cells stained with porous gold−PI conjugate and solid gold−PI conjugates. A, B, and C correspond to the phase contrast image, fluorescent image, and the superimposed image of porous gold−PI stained cells, respectively, while D, E, and F correspond to solid gold−PI stained cells in the same order.

reaction yielded Au:Ag ratios of 1:11.33, 1:4.46, and 1:0.9, respectively. It is clear that even after 5 h of reaction, there is still a fair percentage of silver in the porous structures. The UV−vis spectrum of this solution (Figure 1A) indicates complete damping of the silver plasmon band at 408 nm at this stage and appearance of a peak at ca. 480 nm. It appears likely that the latter peak is due to a silver−gold alloy phase, as inferred earlier.

The highly porous gold nanospheres observed to form in the transmetalation reaction described above (Figures 2C, 2D, and 3) suggest an enhanced surface area for these structures relative to solid gold nanospheres of similar size. The exposed surface area in porous Au NPs obtained by the dialysis membrane procedure outlined above (12.5 kDa cutoff bag, 5×10^{-5} M $HAuCl_4$ and 5 h of reaction; porous Au NPs shown in Figures 2C and 2D) and solid Au NPs was estimated by binding of the well-known fluorescent molecule, propidium iodide (PI). PI is a standard fluorophore used in the imaging of dead cells and, thus, in distinguishing between live and dead cells in a culture medium. PI yields a strong fluorescence emission at 590 nm when excited at 485 nm.[23] Here, we have used the fluorescence intensity of unbound PI in the supernatant after reaction with the porous gold nanospheres (structures shown in Figures 2C and 2D) and solid Au NPs of comparable size as a measure of the surface area in both cases (supernatant obtained by centrifugation of the nanoparticle solution after mixing with 5 mg/mL PI). It is evident that the PI fluorescence signal in the supernatant is significantly reduced in the porous gold nanosphere case (bar III, Figure 2F) relative to solid Au NPs (Figure 2F, bar II), indicating enhanced PI loading in the former. The enhanced binding of PI to the porous gold particles over that of solid gold particles is also evident from the confocal microscopy images recorded from the fixed CHO cells stained with PI conjugated with the respective nanoparticles (Figure 5; A,D correspond to phase images; B,E to fluorescence images; C,F to their superposition recorded from fixed CHO cells after exposure to PI-conjugated porous and solid Au NPs, respectively). The cells stained with PI−porous nanogold conjugates show a significantly enhanced fluorescence (Figures 5B and 5C) in comparison with the cells stained with PI−solid gold conjugates (Figures 5E and 5F). The increase in the fluorescence due to enhanced binding with porous Au NPs was also quantified using FACS analysis (FACS Vantage instrument, Becton-Dickinson, Canada) (data not shown), which indicated a 5-fold increase in the mean fluorescence intensity (MFI) for equal number of cells analyzed after staining with PI−porous gold relative to PI−solid gold conjugates.

As an afterthought, we decided to expose live CHO cells (phase contrast confocal microscopy image of the cells shown in Figure 6A) to PI-loaded porous Au NPs. To our surprise, we observed that when conjugated with the porous nanostructures, PI readily entered live CHO cells as well (Figure 6B). To eliminate the possibility of cell death following exposure to the PI-labeled porous gold nanostructures, the same cell population was subsequently stained with Hoechst stain which is known to specifically stain only live cells (Figure 6C).[24] Thus, the cells which show blue fluorescence under the confocal microscope (Figure 6C) are identified as live CHO cells. Superposition of the fluorescence confocal microscopy images recorded from the live CHO cells after staining with PI-labeled porous gold nanoparticles (Figure 6B, red emission) and Hoechst (Figure 6C, blue emission) results in the image shown in Figure 6D; it is clear from this image that there is significant overlap of the blue and red regions, indicating that the cells into which the PI loaded onto the porous gold nanospheres had entered are indeed alive and viable. The viability of the CHO cells was also established after porous gold−PI treatment by dye exclusion

(23) Jones, K. H.; Senft, J. A. *J Histochem. Cytochem.* **1985**, *33*, 77.

(24) Asakura, A.; Rudnicki, M. A. *Exper. Hematol.* **2002**, *30*, 1339.

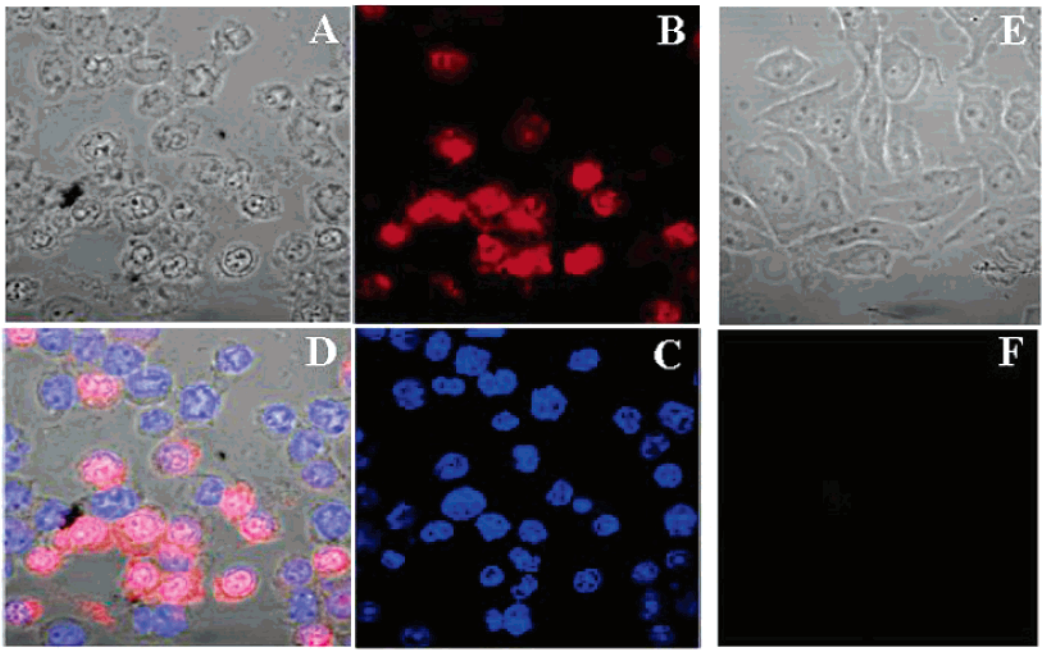

Figure 6. Confocal microscopy images of live CHO cells stained with porous gold−PI conjugate followed by Hoechst staining for checking cell viability. A and B correspond to the phase contrast and fluorescence images respectively of CHO cells stained with porous gold PI conjugate material. Subsequent staining with Hoechst gives blue fluorescence from live CHO cells [C] while superposition of images B and C is shown in D. E and F correspond to the phase contrast and fluorescent images respectively of live CHO cells stained with pure PI.

of trypan blue stain where the live cells do not facilitate the entry of trypan blue (data not shown). On the other hand, live CHO cells (phase contrast confocal microscopy image shown in Figure 6E) incubated with PI alone did not show any fluorescence (Figure 6F), indicating the inability of pure PI to enter the live cells. Thus, the porous gold nanostructures facilitate the uptake of PI in live cells and could therefore provide a novel way of live cell staining. While the exact reason for this unusual result are not clear at this stage, we speculate that it could be due to preferential binding of PI to the inner regions of the pores in the nanostructures. Thus, the PI molecules would not be "seen" by the cells and could enter by an endocytotic pathway along with the porous gold nanosphere carrier. Differences in composition (Au:Ag ratio) at different points in the porous structure could aid in differential binding of PI within the structures.

Although the porous gold nanospheres obtained in this study are similar to those obtained by Xia et al.,[17] the novelty of our approach lies in the fact that we are able to control the kinetics of the transmetalation reaction at room temperature to observe the various stages leading to the generation of porous nanospheres in a single experiment. Furthermore, the use of a dialysis bag obviates the need to purify/separate the end products, enabling precise control and termination of the reaction at any stage by simply removing the dialysis bag from the chloroauric acid solution. This method may be extended to other nanoparticles morphologies as a means of tuning the optical properties. The enhanced surface area make the porous nanospheres ideal candidates for immobilization of biologicals such as proteins and drug molecules and also make it a better contrast-enhancing agent in cell-staining protocols.

Acknowledgment. S.S. and M.B. thank the Council of Scientific and Industrial Research (CSIR) and the Department of Biotechnology, Govt. of India, respectively for financial assistance. A.P. thanks the director, NCL Pune, for permission to carry out research at NCL Pune.

Supporting Information Available: TEM images of borohydride-reduced Au NPs (S1) and TEM and UV−vis−NIR spectroscopy studies of the transmetalation reaction between Ag NPs and gold ions under different conditions (S2). This material is available free of charge via the Internet at http://pubs.acs.org.

CM051165F